The 2013 World Congress on
Advances in Structural Engineering and Mechanics (ASEM13)
Jeju, Korea, September 8-12, 2013

A new numerical modelling for 3D mooring cable fastening a spherical buoy

Xiangqian Zhu[1)], Kun Woo Kim[1)] and *Wan Suk Yoo[2)]

[1), 2)] *School of Mechanical Engineering, Pusan National University, Busan 609-735, Korea*
[2)] wsyoo@pusan.ac.kr

ABSTRACT

Mooring cable system is widely applied in marine engineering to stabilize the floating facilities. Traditionally, a mooring cable is divided into finite elements, and the element-fixed coordinate system is defined by the normal and the tangential vectors of cable geometry, and spline function is employed at each simulation step to carry out the geometry of cable. Profiting from the expression of hydrodynamic drag forces, a new element-fixed coordinate system is developed in this paper. The novelty lies in the combination of relative velocity of fluid in constructing the element-fixe[1]d coordinate system. Without the calculation of spline function, this numerical modelling is effective and suit for the mooring cable tensioned by buoyancy and own gravity. This modelling also simplified the rotational transformation matrix and formulation of hydrodynamic drag forces which are primary among external loads. The stiffness and damping of cable, apparent weight, hydrodynamic drag forces, effect of added mass, and Froude-Krylov force are considered during formulating this numerical modelling. Two mooring cable modelling developed through this element-fixed coordinate system are verified by comparison with the commercial simulation code ProteusDS. One of the modelling stands constant external forces, while the other is connected to a spherical buoy which provides variable buoyancy. The simulation results from these two numerical modelling match well with the results from ProteusDS.

1. INTRODUCTION

The mooring cable system is widely used in marine engineering such as oil and gas production facility, and offshore floating wind turbine (Driscoll and Nahon 1996 and Zhu et al. 2012). Due to the complexity of ocean environment and tremendous size of the floating facilities, mooring cables suffer several kinds of forces which can be separated into three parts, the first part implements along the geometry of cable, such as material stiffness and damping forces; the second part depends on the velocity of fluid with

Note: Copied from the manuscript submitted to “Ocean Systems Engineering, An International Journal” for presentation at ASEM13 Congress

respect to cable, such as the hydrodynamic drag forces which are primary external loads; the third part is gravitational forces which is easily carried out in GCS (global coordinate system). In order to numerically study the motion of cable, the development of numerical modelling of mooring cable starts from inextensible lumped linear elements by Walton and Polachek (1960) to extensible lumped-mass-and-spring modelling by Huang (1994). The lumped-mass-and-spring modelling discretizing mooring cable into finite linear elements obtains widely acceptance in large floating platform system and towed system (Kim et al. 2012). It's known to all that the construction of ECS aims at easily expressing internal and external forces acting on the cable, and these forces are related to GCS through rotational transformation matrix. Traditionally, the ECS is built by the normal and the tangential vectors which are based on the continuous curve function (Bauchau, 2010 and Lee et al. 2012). Cubic-spline function is widely used for the calculation of ECS as shown in DSA, ProteusDS theory and validation (2012). This ECS is convenient in expressing the first part of forces, but limited in the expression of the second part of forces such as drag forces. The drag forces are divided into three parts by the angle between relative velocity and cable geometry. Since this angle has no relation with the ECS, the calculation is complicate and increases inaccuracy. A new ECS taking advantage of the expression of hydrodynamic drag forces is established in this paper. This new ECS is defined by element position vector and relative velocity vector as shown in Fig. 2. The participation of element position vector keeps the advantage in expressing forces along cable. While, due to the participation of relative velocity vector, the angle between relative velocity and cable geometry can be easily converted by the three axial vectors of ECS which can be referred in Eq. (19). What's more, hydrodynamic drag forces are divided into two components in the y-z plane. Not only the first part forces but also the second part is easily expressed with respect to this new ECS. In addition, the normal and tangential vectors are carried out based on the continuous cable in traditionally ECS, while the lumped-mass-and-spring modelling is based on discretized assumption. This complicates the calculation of rotational transformation matrix in traditional ECS (Buckham et al. 2003). The participation of element position vector also simplifies the calculation of transformation matrix by Nikavesh (1988). This new ECS is more compact and efficient than the traditional ECS. Since the application of cable modelling in this paper intends for floating platform, the effects of Froude-Krylov should not be ignored as towed marine system by (Buckham et al. 2003) and (Hover et al. 1994) did. Deriving from Morison's equation, the effects of Froude-Krylov are also considered during formulating of the numerical modelling of the mooring cable by Liu and Bergdahl(1996) and Yu and Tan (2006). The stiffness and damping of cable, apparent weight, hydrodynamic drag forces, effects of added mass, and Froude-Krylov force are considered during building this numerical modelling of mooring cable. Due to the limitation of experiment equipments, the accuracy of this new ECS is verified by comparison with simulation code ProteusDS of which the cable is based on cubic-spline lumped mass modelling. Two numerical modelling of cable which stand surface waves, currents and external forces are created in this paper. The external forces are provided through two ways, one cable stands constant external forces acting on the first node and the other stands variable buoyancy which are provided by the submerged part of floating spherical buoy of which the bottom is connected with the

first node of cable as shown in Fig.1. The simulation results from this numerical modelling built by this new ECS match well with the results from ProteusDS.

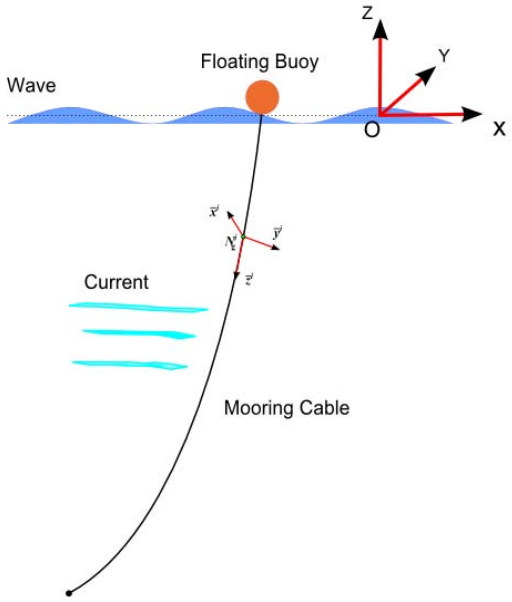

Fig. 1 The coordinate system of mooring cable fastening a floating buoy

2. OCEAN MODELLING

The linear wave theory is used in this paper to express the propagation of surface waves by Journeer and Massie (2001). The elevation of free surface wave is the superposition of each independent propagation wave as is shown in Eq. (1). The parameters of the ocean states for verifying modelling are listed in Table. 1.

$$\zeta = \sum \zeta_a \cos(kx - \omega t) \tag{1}$$

With the assumption of infinity of water depth, the velocities and accelerations of the water particles can be carried out according to three axles and are shown in Eq. (2) and (3) respectively.

$$\begin{aligned} u_g &= \zeta_a^x \cdot \omega^x \cdot e^{k^x Z_g} \cos(k^x X_g - \omega^x t) \\ v_g &= \zeta_a^y \cdot \omega^y \cdot e^{k^y Z_g} \cos(k^y Y_g - \omega^y t) \\ w_g &= \zeta_a^x \cdot \omega^x \cdot e^{k^x Z_g} \sin(k^x X_g - \omega^x t) + \zeta_a^y \cdot \omega^y \cdot e^{k^y Z_g} \sin(k^y Y_g - \omega^y t) \end{aligned} \tag{2}$$

$$\dot{u}_g = \zeta_a^x \cdot (\omega^x)^2 \cdot e^{k^x Z_g} \sin(k^x X_g - \omega^x t)$$
$$\dot{v}_g = \zeta_a^y \cdot (\omega^y)^2 \cdot e^{k^y Z_g} \sin(k^y Y_g - \omega^y t) \quad (3)$$
$$\dot{w}_g = -\zeta_a^x \cdot (\omega^x)^2 \cdot e^{k^x Z_g} \cos(k^x X_g - \omega^x t) - \zeta_a^y \cdot (\omega^y)^2 \cdot e^{k^y Z_g} \cos(k^y Y_g - \omega^y t)$$

where the wave number k and wave angular velocity ω are defined as following,

$$L_g = \frac{|g| T_g^2}{2\pi} \quad (4)$$

$$k = \frac{2\pi}{L_g} \quad (5)$$

$$\omega^2 = k|g| \quad (6)$$

The current is treated as a constant velocity in this paper as shown in Table 1. Finally the velocity of the fluid is expressed as Eq. (7) where $\underline{V}_g^w = [u_g, v_g, w_g]^T$

$$\underline{V}_g^f = \underline{V}_g^w + \underline{V}_g^c \quad (7)$$

Table 1. The ocean state

Parameter	*Magnitude*	*Unit*
ζ_a^x	0.35	m/s
ζ_a^y	0.6	m/s
T_a^x	6.4	s
T_a^x	8	s
$\underline{V}_g^c$	[1; 0; 0]	m/s
ρ_f	1025	kg/m^3

2. NEW CABLE MODELLING

The origin of the GCS locates in still water level (SWL), X-axis directs east while the positive of Z-axis is vertical upward, and right handed coordinate system implies Y-axis directing north. The mooring cable is discreted into $(N-1)$ finite elements ordered from top to bottom, and the mass of cable is lumped on N nodes. The position of i^{th} node is

expressed by a column vector $\underline{N}_g^i$ with respect to the GCS. Since the cable fastening the floating platform is relative stable compared to the cable towing a marine vehicle, $\underline{V}_g^R$ is defined as the velocity of fluid with respect to the velocity of cable at the element center. The construction of ECS is illustrated in Fig. 2.

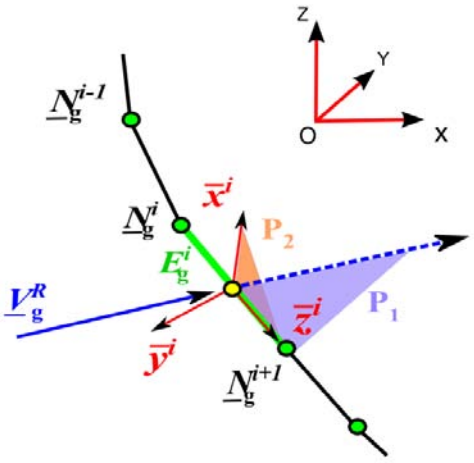

Fig. 2 The element-fixed coordinate system of mooring cable

$$\underline{E}_g^i = \underline{N}_g^{i+1} - \underline{N}_g^i \tag{8}$$

$$\underline{V}_g^i = \underline{V}_g^f - \dot{\underline{N}}_g^i \tag{9}$$

The element velocity $\underline{V}_g^R$ is carried out by the velocities of i^{th} and $(i+1)^{th}$ nodes. Notation $\dot{\underline{N}}_g^i$ indicates a derivative of displacement of i^{th} node $\underline{N}_g^i$ with respect to time t.

$$\underline{V}_g^R = \frac{\underline{V}_g^{i+1} + \underline{V}_g^i}{2} \tag{10}$$

The three unit vectors of ECS for element are defined respectively in Eq. (11).

$$\begin{aligned} \bar{z}^i &= \frac{\underline{E}_g^i}{\| \underline{E}_g^i \|} \\ \bar{x}^i &= \frac{\tilde{z}^i \underline{V}_g^R}{\| \tilde{z}^i \underline{V}_g^R \|} \\ \bar{y}^i &= \tilde{z}^i \bar{x}^i \end{aligned} \tag{11}$$

What should be pointed out is the singularity of $\overline{x}^i$ when $\underline{V}_g^R = 0$. In order to validate the ECS in this special case, the minimum magnitude of $\underline{V}_g^f$ is 0.0001 instead of 0 at initial condition. It is acceptable in the real case due to the complexity of ocean environment.

One of the advantages of this definition of the ECS comes out in the expression of rotational transformation matrix $\underline{\underline{A}}^i$. The unit vectors $\overline{x}^i$, $\overline{y}^i$ and $\overline{z}^i$ are used instead of calculating of rotation angles by Huang (1994) and Buckham et al. (2003).

$$\underline{\underline{A}}^i = [\overline{x}^i, \overline{y}^i, \overline{z}^i] \tag{12}$$

2.1 Material Tension

Due to the elastic behavior of cable, the inner forces can be divided into material tension and the material damping by Huang (1994). The tension $\underline{T}_b^i$ within i^{th} element exists along $\overline{z}^i$ and depends on the axial stiffness E and strain ε_b^i.

$$\underline{T}_b^i = \frac{\pi d_c^2}{4} E \varepsilon_b^i \overline{z} \tag{13}$$

where d_c is the diameter of the cable. The axial strain ε_b^i is defined as following:

$$\varepsilon_b^i = \frac{l^i - l_0^i}{l_0^i} \tag{14}$$

where l_0^i means the unstretched length of i^{th} cable element, while l^i means the element length in current simulation step.

$$l^i = \sqrt{\underline{E}_g^{iT} \underline{E}_g^i} \tag{15}$$

2.2 Material Damping

The material damping within element is defined as a liner function of velocity difference between element-terminal nodes along $\overline{z}^i$ axis.

$$\underline{D}_b^i = C_d \underline{\underline{A}}^{iT} (\dot{N}_g^{i+1} - \dot{N}_g^i) \overline{z} \tag{16}$$

where $\underline{\underline{A}}^{iT}$, the transposed matrix of $\underline{\underline{A}}^i$ aids to converting the velocity difference from GCS to ECS, $\overline{z} = [0,0,1]^T$ indicates that the material damping exists along z-direction of the GSC. C_d represents the damping coefficient depending on the material.

2.3 Hydrodynamic Drag Force

The hydrodynamic drag forces are primary forces acting on the cable. Since the ECS is constructed by relative velocity $\underline{V}_g^R$, the advantage is illustrated again in the expression of hydrodynamic drag forces $\underline{F}_D^i$. The vector of hydrodynamic forces is divided into two components in the y-z plane with respect to ECS.

$$\underline{F}_D^i = \underline{F}_z^i + \underline{F}_y^i \tag{17}$$

According to the definition, the drag forces are quadratic of relative velocity of fluid and are divided into lengthwise and transverse two components as shown in Liu and Bergdahl (1996) and Yu and Tan (2006).

$$\begin{aligned} \underline{F}_z^i &= \frac{\pi}{2} C_f \rho_f d^i l^i \| \underline{V}_g^R \|^2 \cos\eta \\ \underline{F}_y^i &= \frac{1}{2} C_n \rho_f d^i l^i \| \underline{V}_g^R \|^2 \sin\eta \end{aligned} \tag{18}$$

where C_n, is drag coefficient in transverse and C_f is the friction coefficient of cable with the surrounding fluid. η represents the angle between relative velocity $\underline{V}_g^R$ and cable element vector $\bar{z}^i$ as shown in Fig. 3, and $0 \le \eta \le \pi$. As we know,

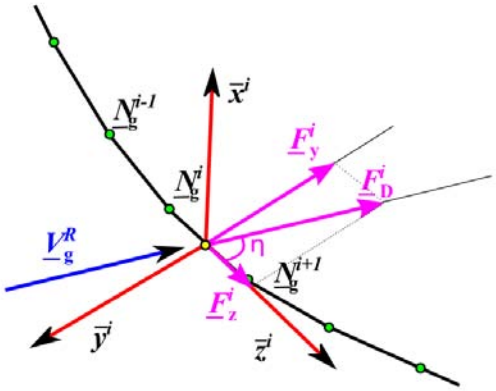

Fig. 3 The drag forces acting on the cable element

$$\begin{aligned} \bar{z}^T \underline{V}_g^R &= \| \underline{V}_g^R \| \cos\eta \\ \tilde{z} \underline{V}_g^R &= \| \underline{V}_g^R \| \sin\eta \bar{x} \\ \tilde{z}(\tilde{z} \underline{V}_g^R) &= \| \underline{V}_g^R \| \sin\eta \bar{y} \end{aligned} \tag{19}$$

Finally, the $\underline{F}_y^i$ and $\underline{F}_z^i$ are illustrated in Eq. (20)

$$\begin{aligned}\underline{F}_z^i &= \frac{\pi}{2} C_f \rho_f d^i l^i \| \underline{V}_g^R \| \overline{z}^T \underline{V}_g^R \cdot \overline{z} \\ \underline{F}_y^i &= \frac{1}{2} C_n \rho_f d^i l^i \| \underline{V}_g^R \| \tilde{z}(\tilde{z} \underline{V}_g^R)\end{aligned} \tag{20}$$

2.4 Apparent Weight

Since the cable is buoyant in fluid, the apparent weight of the i^{th} cable element $\underline{F}_W^i$ equals the difference between gravitational force and buoyancy. $\underline{g}$ means the gravitational acceleration vector $\left[0, 0, -9.81\right]^T$.

$$\underline{F}_w^i = (m_c^i - m_a^i)\underline{g} \tag{21}$$

where

$$\begin{aligned} m_c^i &= \frac{\pi d_c^2}{4} l^i \rho_c \\ m_a^i &= \frac{\pi d_c^2}{4} l^i \rho_f \end{aligned} \tag{22}$$

2.5 Added-mass and Froude-Krylov Effects

Added mass represents the pressure effects due to the relative acceleration between wave particles and cable, and Froude-Krylov force represents the pressure effects due to undisturbed incident waves. The cable modelling in this paper intends for floating platform which is stable compared with towed marine vehicle, so the effects caused by incident wave should not be ignored. Deriving from Morison's equation, the effects of added-mass and Froude-Krylov are shown in Eq. (23).

$$\underline{f}_A^i = (1 + C_A) m_a^i \dot{\underline{V}}_g^f - C_A m_a^i \ddot{\underline{N}}_g^i \tag{23}$$

where C_A is the coefficient of added-mass normal the geometric of cable, $\dot{\underline{V}}_g^f$ is the acceleration of surrounding fluid particles, and $\ddot{\underline{N}}_g^i$ represents the acceleration of cable node. Combining the added-mass effects with the mass matrix, the modified mass matrix is shown in Eq. (24).

$$M^i = \begin{bmatrix} m_c^i + C_A m_a^i & 0 & 0 \\ 0 & m_c^i + C_A m_a^i & 0 \\ 0 & 0 & m_c^i \end{bmatrix} \tag{24}$$

And the modified Froude-Krylov force is

$$\underline{F}_A^i = (1+C_A) m_a^i \dot{\underline{V}}_g^f \tag{25}$$

2.6 Governing Equation

The governing equation is defined according to the N nodes of mooring cable, and the forces acting on each cable element are divided equally on the element-terminal nodes. The governing equation for nodes except endpoints of cable is defined as below:

$$\begin{aligned} M^i \ddot{\underline{N}}_g^i = \underline{\underline{A}}^i (\underline{T}_b^i + \underline{D}_b^i + \frac{1}{2}\underline{F}_D^i) + \frac{1}{2}(\underline{F}_A^i + \underline{F}_W^i) - \\ \underline{\underline{A}}^{i-1} (\underline{T}_b^{i-1} + \underline{D}_b^{i-1} - \frac{1}{2}\underline{F}_D^{i-1}) + \frac{1}{2}(\underline{F}_A^{i-1} + \underline{F}_W^{i-1}) \end{aligned} \tag{26}$$

The bottom of the cable is assumed to be fixed with seabed in this numerical modelling. The first node of the cable is connected with the floating platform which provides an external force $\underline{F}_{ext}^1$ on the cable.

3. VERIFICATION

The verification of this numerical modelling was implemented through two modelling which stand the surface wave, current and external forces $\underline{F}_{ext}^1$. The differences lie in the way in which $\underline{F}_{ext}^1$ applied. The first modelling uses constant forces while a floating sphere is implemented to provide variable $\underline{F}_{ext}^1$ in the second modelling. The displacements of cable nodes and tensions within elements were compared with simulation results from ProteusDS. The modelling of mooring cable fastening a floating sphere in ProteusDS is shown in Fig. 4.

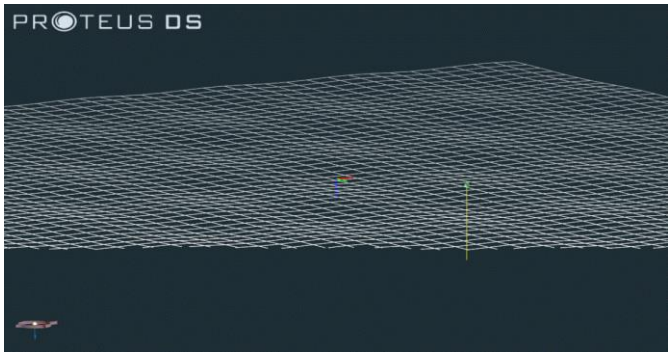

Fig. 4 The modelling of mooring cable fastening floating buoy in ProteusDS

3.1 Constant Forces

The mooring cable is divided into 10 elements by 11 nodes in this modelling and suffers propagation wave in X- and Y-direction, ocean current in X-direction of which the value can be referred in Tab. 1. The external forces are applied on the first node of cable with constant values $\underline{F}_{ext}^{1} = [0, 0, 600]^{T}$. The tension within the first element is shown in Fig 5. The mean value of tension from MATLAB modelling is almost the same with that from ProteusDS; In addition, MATLAB modelling has slight vibration according to the motion of the cable which properly reflects the reality. The displacements of the whole mooring cable from MATLAB codes match well with the results from ProteusDS which is shown in Figs. 6-8.

Table 2. The property of cable

Parameter	*Magnitude*	*Unit*
d_c	0.03	m
ρ_c	1570	kg/m^3
E	2.38e9	N/m^2
C_d	1.5	
C_n	1	
C_f	0.03	
C_A	1	
$\underline{N}_g^1$	[0;0;-2]	
$\underline{N}_g^N$	[0;0;-30]	

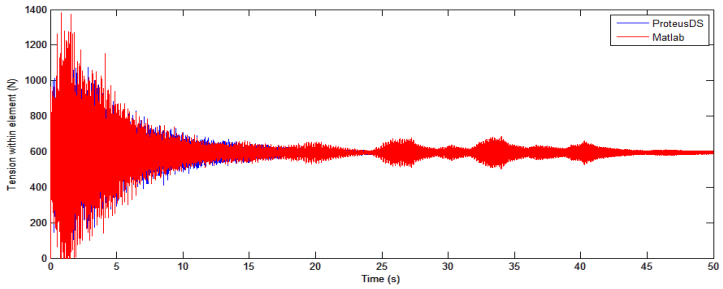

Fig. 5 Tension within the first element

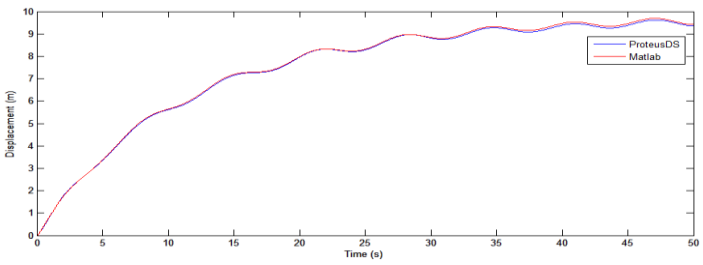

Fig. 6 The displacement of the first node along X-direction

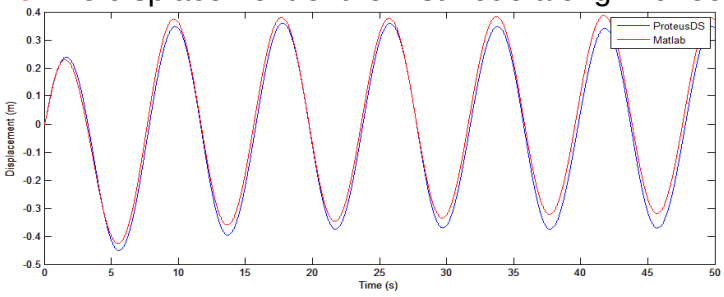

Fig. 7 The displacement of the first node along Y-direction

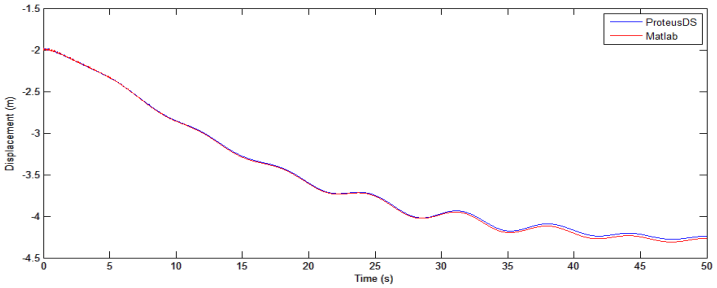

Fig. 8 The displacement of the first node along Z-direction

3.2 Spherical Buoy

The sphere modelling developed in this paper simulates floating platform and provides external forces which avoids sinking of cable. The geometry data of the sphere is shown in Table. 3. Due to the symmetrical geometry of sphere, the rotation is ignored during developing sphere modelling, and the displacement of sphere is carried out by the geometrical relationship between sphere and cable. The displacement of cable node $\underline{N}_g^1$ is the same with the bottom of the sphere. Three points a , b and c respectively are fixed in the sphere cross-section which cross the center of the sphere and is parallel with the SWL. These three points located impartially on the edge of concentric circle of which the radius is R_p . The symbol ζ_g^a , ζ_g^b and ζ_g^c represent the surface wave elevation at points a , b and c respectively which are illustrated detail in Fig. 9.

Table 3. The property of buoy

Parameter	*Magnitude*	*Unit*
R	1	m
R_p	0.5	m
M_s	10	kg

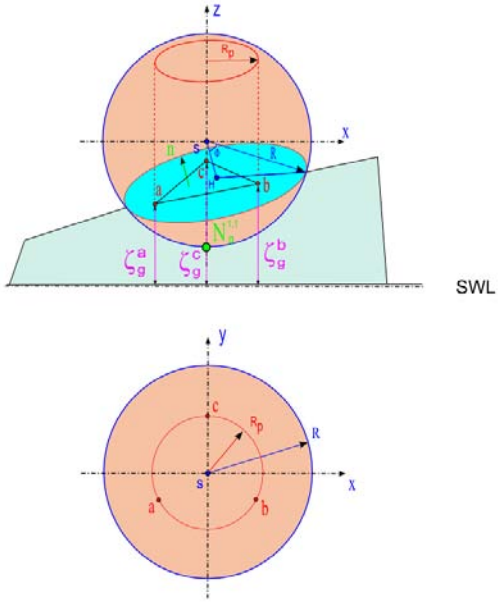

Fig. 9 Numerical modelling of floating buoy

$$\begin{aligned}
\zeta_g^a &= \zeta_a^x \cos(k^x(N_g^{1,1} - \frac{\sqrt{3}}{2}R_p) - \omega^x t) + \zeta_a^y \cos(k^y(N_g^{1,2} - \frac{1}{2}R_p) - \omega^y t) \\
\zeta_g^b &= \zeta_a^x \cos(k^x(N_g^{1,1} + \frac{\sqrt{3}}{2}R_p) - \omega^x t) + \zeta_a^y \cos(k^y(N_g^{1,2} - \frac{1}{2}R_p) - \omega^y t) \\
\zeta_g^c &= \zeta_a^x \cos(k^x N_g^{1,1} - \omega^x t) + \zeta_a^y \cos(k^y(N_g^{1,2} + R_p) - \omega^y t)
\end{aligned} \tag{27}$$

The position vectors of these three points are carried out with respect to GCS. Unitize the axial component of normal vector of this cross-section and represented by $[n_{x,}n_y,n_z]$ which illustrates the direction of buoyancy.

$$[n_{x,}n_y,n_z] = \frac{\underline{ac} \times \underline{bc}}{\| \underline{ac} \times \underline{bc} \|} \tag{28}$$

where,

$$\underline{ac} = \left[\frac{\sqrt{3}}{2} R_p, \frac{3}{2} R_p, \zeta_g^c - \zeta_g^a \right]^T$$
$$\underline{bc} = \left[-\frac{\sqrt{3}}{2} R_p, \frac{3}{2} R_p, \zeta_g^c - \zeta_g^b \right]^T \quad (29)$$

Since the length of wave is much larger than the radius of sphere R, the wetted cross curve is simplified as a plane, and the distance from the center of sphere to the cross plane SH is shown in Eq. (30).

$$SH = (n_x \cdot \frac{\sqrt{3}}{2} R_p + n_y \cdot \frac{1}{2} R_p + n_z \cdot (\underline{N}_g^{1,3} + R - \zeta_g^a)) \quad (30)$$

The submerged volume V_s is carried out through Eq. (31) with respect to the spherical coordinate.

$$V_s = \int_0^{2\pi} d\theta \int_0^{\phi} \sin\phi d\phi \int_0^R r^2 dr - \frac{1}{3} SH(R^2 - SH^2) \quad (31)$$

where 2ϕ is corner angle of the composed cone.

$$\phi = \arccos \frac{SH}{R} \quad (32)$$

Since this paper focuses on the numerical modelling of mooring cable, the external loads acting on the 1^{st} node of cable is composed by buoyancy and gravitational force. Taking advantage of the symmetrical geometry of sphere, the buoyancy always directs the center of sphere during the simulation and can be divided into three axial directions. The gravitational force is constant and depends on the mass of sphere M_s. Finally, X-component, Y-component and Z-component of the external loads $\underline{F}_{ext}^1$ are shown in Eq. (33).

$$F_{ext}^{1,1} = V_s \rho_f \mid g \mid n_x$$
$$F_{ext}^{1,2} = V_s \rho_f \mid g \mid n_y \quad (33)$$
$$F_{ext}^{1,3} = V_s \rho_f \mid g \mid n_z - M_s \mid g \mid$$

This modelling is developed for the validation of variable external loads. The floating spherical buoy provides variable buoyancy acting on the first node of the mooring cable. This first node of mooring cable is connected with the bottom of the buoy and locates at

$[0,0,0]$ initially. The ocean state and the property of mooring cable are the same with the first modelling which can be referred in Tables. 1-2. The spherical buoy is submerged by the superposition of the wave crests at initial condition and gradually, gets stable around the equilibrium position, so the tension vibrates largely at the beginning which is shown in Fig. 10. The displacement of buoy in Z-direction also achieves maximum near the beginning as shown in Fig. 13. Generally, the displacements of the first nodes in MATLAB code match well with those from ProteusDS as shown in the Figs. 11-13. What's more, the MATLAB code is more actual than ProteusDS in the expression of tension and displacement of cable in Z-direction. Especially, the tension is unreasonable around 26 second in ProteusDS as shown in Fig. 10. These show the advantages of this new GCS.

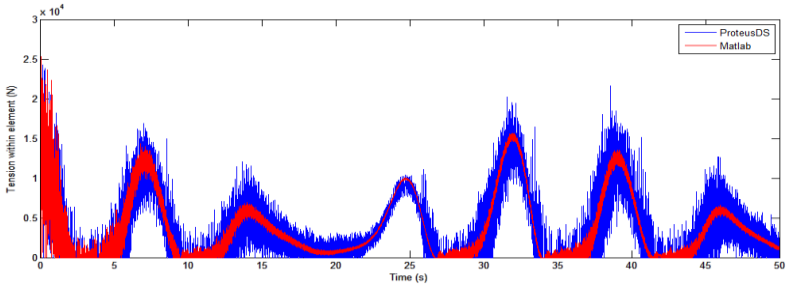

Fig. 10 Tension within the first element

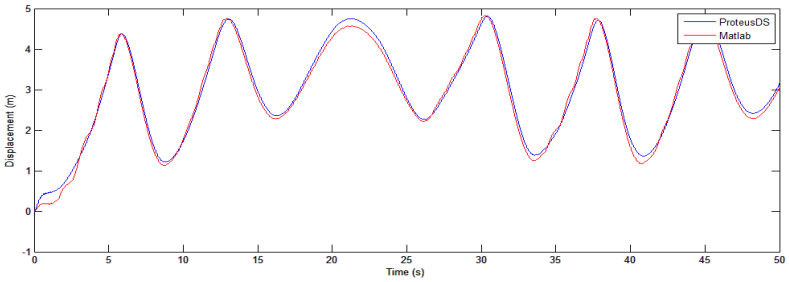

Fig. 11 The displacement of the first node along X-direction

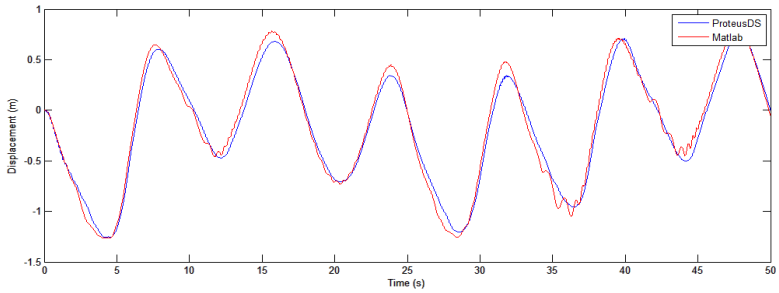

Fig. 12 The displacement of the first node along Y-direction

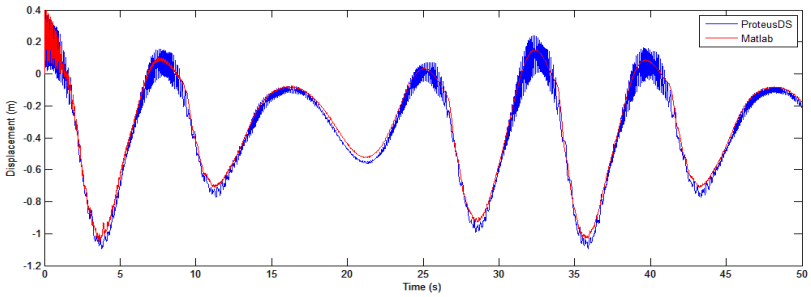

Fig. 13 The displacement of the first node along Z-direction

4. CONCLUSIONS

In this paper, a new element-fixed coordinate system is developed based on the relative velocity of fluid and the geometry of mooring cable. Both the rotational transformation matrix and hydrodynamic drags are simplified with this coordinate system. This cable modelling considers the stiffness and damping of cable, apparent weight, hydrodynamic drag forces, effect of added mass, and Froude-Krylov force. Due to the limitation of experiment conditions, this modelling was verified by two numerical modelling which match well with the results from ProteusDS. The numerical spherical buoy is also well developed; the construction method could give reasonable experience for the calculation of submerged volume.

5 ACKNOKLEDGMENT

This work was supported by the Korea Institute of Energy Technology Evaluation and Planning(KETEP) grant(No. 20113020020010) funded by the Korea government Ministry of Knowledge Economy.

REFERENCES

Driscoll, R., Nahon, M. (1996), “Mathematical modeling and simulation of a moored buoy system”, *IEEE,* 517-523.

Zhu, X.Q., Kim, H.W. and Yoo, W.S. (2012), “Dynamic analysis of an offshore wind turbine with a spar-type platform”, *The 6th Asian conference on Multibody Dynamic*, Shanghai, China.

Walton, T.S. and Polachek, H. (1960), “Calculation of transient motion of submerged cables”, Mathematics of Computation 14(69), 27-46.

Huang, S. (1994), “Dynamic analysis of three-dimensional marine cable”, Ocean Engineering 21(6), 587-605.

Kim, K.W., Lee, J.W. and Yoo, W.S. (2012) “The motion and deformation rate of a flexible hose connected to a mother ship”, Journal of Mechanical Science of Technology 26(3), 703-710.
Bauchau, O.A. (2010), “Flexible Multibody Dynamic”, Springer, Solid Mechanics and Its Application, 176, 613-689.
Lee, J.W., Kim, K.W., Kim, H.R. and Yoo, W.S. (2012), “Prediction of unwinding behavior and problems of cables from inner-winding spool dispensers”, Nonlinear Dynamics, 67, 1791-1809
DSA Pacific, (2012), “ProteusDS theory and validation”, Dynamic system analysis Ltd.
Buckham, B., Nahon, M., Seto, M., Zhao, X. and Lambert, C. (2003), “Dynamic and control of a towed underwater vehicle system, Part I: Model Development”, Ocean Engineering, 30, 453-470
Nikavesh, P. E. (1988), “Computer-aided analysis of mechanical systems”, PRENTICE HALL, Englewood Cliffs, New Jeresey.
Hover, F.S., Grosenbaugh, M.A. and Triantafyllou (1994), “Calculation of dynamic motions and tensions in towed underwater cables”, IEEE Journal of Ocean Engineering, 19(3) 449-457
Liu, Y. G. and Bergdahl, L. (1996), “Influence of current and seabed friction on mooring cable response comparison between time-domain and frequency-domain analysis”, ElSEVIER, Engineering Structures Vol. 19, No. 11, 945-953
Long, Y. and Tan, J. H. (2006), “Numerical investigations of seabed interaction in time domain analysis of mooring cables”, Journal of Hydrodynamics, Ser. B, 18(4), 424-430
Karimirad, M. (2011), “Stochastic dynamic response analysis of Spar-type wind turbines with catenary or taut mooring systems”, Thesis for the degree of doctor of philosophy, Norwegian University of Science and Technology.
Journee, J.M.J. and Massie, W.W., (2001), “Offshore Hydromechanics”, Delft University of Technology, First Edition, Chapter 5
Buckham, B. J. (1997), “Dynamics modelling of low-tension tethers for submerged remotely operated vehicles”, Thesis for the degree of doctor of philosophy. University of Victoria.
Mavrakos, S.A., Papazoglou, V.J., Triantafyllou, M.S. and Hatjigeorgiou, J. (1996), “Deep water mooring cable”, ElSEVIER, Marine Structures 9, 181-209
DSA Pacific, (2011), “ProteusDS 2011 Manual”, Dynamic System Analysis Ltd.
DSA Pacific, (2011), “ProteusDS 2011 Tutorials”, Dynamic System Analysis Ltd. Version 1.0